Dalton Transactions

Accepted Manuscript

This article can be cited before page numbers have been issued, to do this please use: W. Schmitt, C. Healy, F. Steuber, P. Wix, L. Macreadie and A. C. Kathalikkattil, *Dalton Trans.*, 2019, DOI: 10.1039/C9DT00075E.

ROYAL SOCIETY OF CHEMISTRY

rsc.li/dalton

Dalton Transactions

View Article Online
DOI: 10.1039/C9DT00075E

ARTICLE

Assembly, Disassembly and Reassembly: a "Top-Down" Synthetic Strategy towards Hybrid, Mixed-Metal {$Mo_{10}Co_6$} POM Clusters

Received 00th January 20xx,
Accepted 00th January 20xx

DOI: 10.1039/x0xx00000x

www.rsc.org/

Colm Healy,[a,b] Friedrich W. Steuber,[a] Paul Wix,[a] Lauren Macreadie,[a,c] Amal Cherian Kathalikkattil[a] and Wolfgang Schmitt[a]

Polyoxometalates (POMs) are commonly prepared using a "bottom-up" synthetic procedure. The alternative "top-down" approach of disassembling a pre-formed POM unit to generate new synthetic intermediates is promising, but relatively comparatively underused. In this paper, a rationale for the top-down method is provided, demonstrating that this approach can generate compounds that are fundamentally inaccessible from simple bottom-up assembly. We demonstrate this principle through the synthesis of a series of 10, new, mixed-metal, hybrid compounds with the general formula $[TBA]_2[Mo^{VI}_{10}Co^{II}_6O_{30}(R_pPO_3)_6(R_cCOO)_2(L)_x(H_2O)_6]$ (TBA = tetrabutylammonium, R_p = phosphonate moiety, R_c = carboxylate moiety, L = pyridyl ligand, and x = 2–4), including a one-dimensional polyoxometalate-based coordination polymer. We propose that these structures are generated from $\{Mo_xO_{3x-1}\}$ fragments that cannot be accessed from bottom-up assembly alone. The POM clusters are stabilised by three distinct classes of organic ligand – organophosphonate, carboxylate and pyridyl ligands – which can each be substituted independantly, thus providing a controlled route to ligand functionalisation.

Introduction

Polyoxometalates (POMs) are a well-studied class of molecular-scale transition metal oxides (typically oxides of vanadium, molybdenum and tungsten). This remarkable class of materials has been studied since the early 1800s, and remain the subject of intensive investigation today.[1] Classical POMs are often able to accept and/or donate multiple electron or proton equivalents without any structural rearrangement; this structural robustness has led POMs to find use in catalytic and charge-transfer applications.[2,3] However, classical POMs are often difficult to modify synthetically, as the oxophilicity of POM metal ions generally hampers the incorporation heterometals or organic ligands.[4,5]

Incorporating heterometals or organic ligands greatly increases both structural diversity and possible applications. POMs which are supported by organic ligands (Hybrid POMs) can be modified post-synthetically, or assembled into supramolecular architectures or frameworks.[6–10] Transition Metal Substituted POMS (TMS-POMs) have increased magnetic and electronic diversity compared to the parent POMs, and notably have been used as catalysts for the highly demanding water oxidation reaction.[11–13] However, synthetic approaches towards either hybrid or TMS-POMs are relatively limited.

Classically, POMs were accessed by "bottom-up" processes, the mechanisms of which were elucidated by Cronin, Poblet and co-workers.[14–16] When aqueous solutions of monomeric $[MO_4]^{n-}$ *oxo*-anions are acidified, a series of protonation, condensation and dehydration steps can generate various molecular POM species. The form of the resulting molecular species is often dependent on a template effect.[17] While certain strategies do exist to produce hybrid or TMS-POMs (*e.g.* the lacunary approach), established methodologies rely significantly on bottom-up approaches.[18–22]

A possible alternative was presented by Cronin *et al.* in 2008. It was demonstrated using mass spectrometry that $[Mo_6O_{19}]^{2-}$ Lindqvist clusters transform *via* "top-down" processes to the β-octamolybdate $[Mo_8O_{24}]^{4-}$. The Lindqvist species disassembles into oligomers which subsequently reassemble to generate the new product.[23]§ Subsequent work by Cronin *et al.* demonstrated that a hybrid TMS-POM, the Anderson-structured $[MnMo_6O_{18}(L)_2]^{3-}$, could be accessed by a similar 'assembly-disassembly-reassembly' process.[24]

However, these studies omit the key realisation that the fragments formed by top-down disassembly are fundamentally different from those that can be accessed by a direct bottom-up assembly approach (Figure 1). Reassembly of these fragments could therefore generate new architectures (particularly hybrid and TMS-POM structures) which are impossible to synthesise *via* direct bottom-up approaches.

[a] School of Chemistry and CRANN, Trinity College Dublin, College Green, Dublin 2, Ireland.
[b] MacDiarmid Institute for Advanced Materials and Nanotechnology, School of Physical and Chemical Sciences, University of Canterbury, Private Bag 4800, Christchurch 8041, New Zealand
[c] CSIRO Manufacturing, Bayview Ave, Clayton, VIC 3168, Australia
Electronic Supplementary Information (ESI) available: Crystallographic details, supplementary characterisation, and additional images. See DOI: 10.1039/x0xx00000x

View Article Online
DOI: 10.1039/C9DT00075E

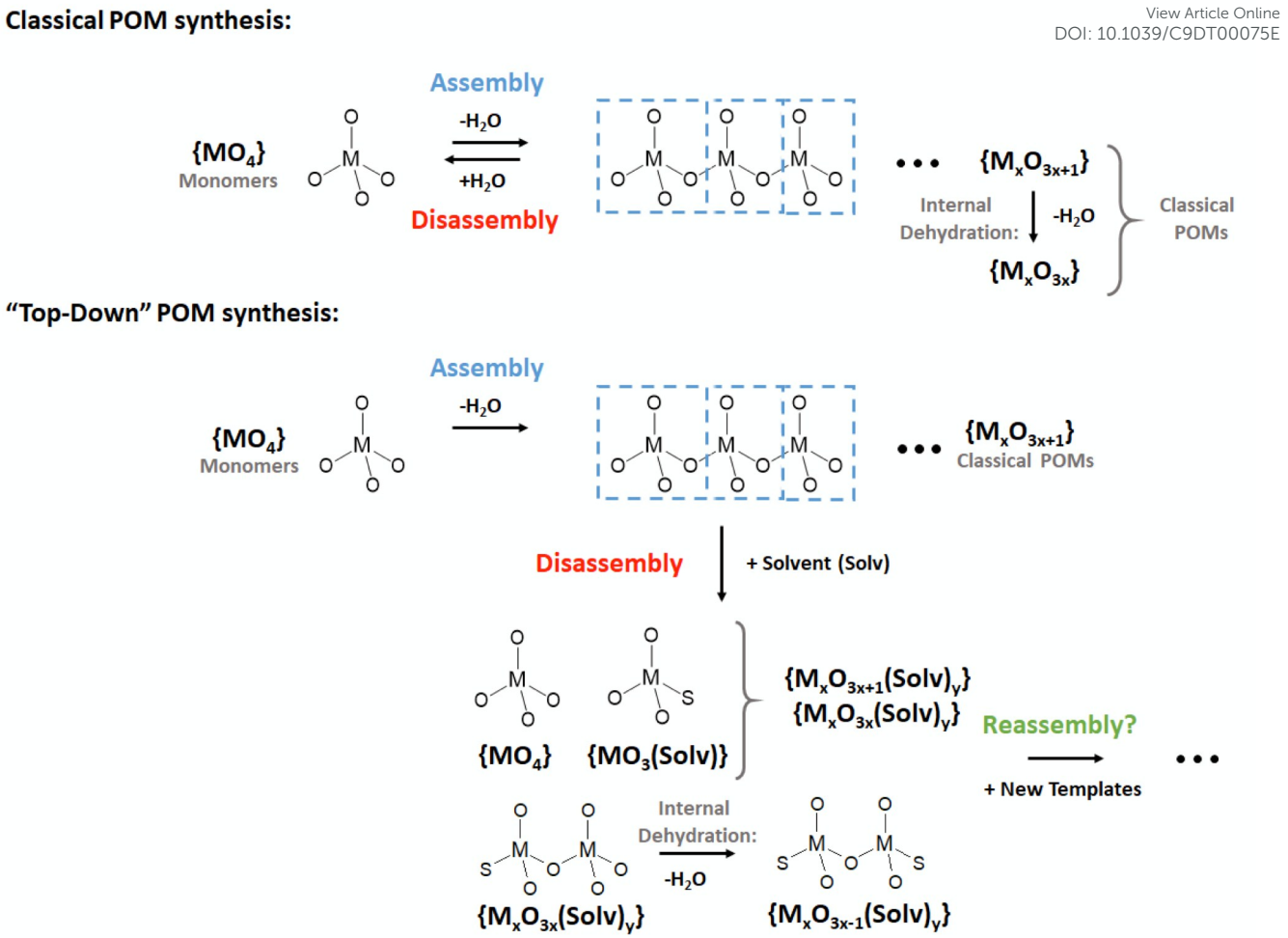

Figure 1. Schematic representation of "bottom-up" and "top-down" approaches to POMs. Classical "bottom-up" assembly of POMs tends to produce compounds of the generic formula $\{M_xO_{3x+1}\}$ or $\{M_xO_{3x}\}$ *via* sequential addition of $\{MO_4\}$ monomers along with loss of water. "Top-down" synthesis subsequently disassembles these compounds in a non-aqueous solvent (Solv), generating a mixture of $\{M_xO_{3x+1}(Solv)_y\}$, $\{M_xO_{3x}(Solv)_y\}$ and $\{M_xO_{3x-1}(Solv)_y\}$ fragments, which are fundamentally different from the fragments accessible by purely bottom-up approaches. These diverse intermediates can be reassembled by the addition of new templates to generate novel hybrid or mixed-metal POM compounds.

We realise that top down synthesis has been fundamentally underexplored since top-down processes were initially demonstrated.[25–29] In particular, top-down strategies to develop novel synthons that can subsequently be reassembled into new architectures are quite rare.[30–33] This methodology has recently been explored by Streb *et al.* in the case of vanadates,[30,31] Nyman *et al.* in the case of niobates,[32] and ourselves in the case of molybdates,[33] but has otherwise been largely absent from the literature.

In this paper, we demonstrate the utility of the top-down strategy to generate novel, structurally interesting, hybrid TMS-POM compounds. We highlight that top-down disassembly processes can generate fragments that are fundamentally different from those that can be accessed *via* bottom-up synthesis, including fragments coordinated by labile solvent molecules and fragments with unusual Mo/O ratios. The strategy was applied to generate a series of mixed-metal, hybrid $\{Mo_{10}Co_6\}$ structures supported by a combination of phosphonate, carboxylate and pyridyl ligands. These organic ligands can be substituted orthogonally to one another, allowing any one organic component to be modified while retaining the rest of the structure. To further demonstrate the utility of the approach, orthogonal ligand substitution was exploited to generate one dimensional polymer structures. Finally, possible templating effects which led to the generation of the $\{Mo_{10}Co_6\}$ structure will be evaluated, and analysed in the context of previously prepared compounds.

Results and Discussion

The Top-Down Synthetic Approach

Classical, "bottom-up" assembly of a POM structure relies on acidification of aqueous solutions of a monomeric metal oxide unit. The specific sequence of mechanistic events can be complicated for a given synthesis, potentially involving a network of converging reaction mechanisms involving large numbers of species in solution at one time – nevertheless, the

View Article Online DOI: 10.1039/C9DT00075F

processes which underly these synthetic procedures have been understood in general terms for some time.[14–16]

Upon acidification, two monomeric metal oxide units can condense with the expulsion of a water molecule:

$$2[MO_4]^{n-} + 2H^+ \rightarrow [M_2O_7]^{n-} + H_2O$$

This process continues to generate oligomeric species:

$$x[MO_4]^{n-} + 2(x-1)H^+ \rightarrow [M_xO_{3x+1}]^{n-} + (x-1)H_2O$$

Dehydration can also occur in an intramolecular fashion:

$$[M_xO_{3x+1}]^{n-} + 2H^+ \rightarrow [M_xO_{3x}]^{n-} + H_2O$$

These generic reaction schemes account for a range of POM formulae; for example, the Lindqvist structure satisfies the $[M_xO_{3x+1}]^{n-}$ formula for x=6, while the Keggin structure satisfies the $[M_xO_{3x}]^{n-}$ formula for x=12 (in the latter case, a structure-directing tetrahedral anion must also be added to the formula). In aqueous solution, disassembly of a POM structure simply follows the reverse pathway, with the addition of water, cleavage of the oligomers, and deprotonation to generate *oxo* ligands. These processes are well understood, and are summarised in Figure 1.[14–16]

Conceptually, the assembly process can be simplified as the addition of $\{MO_3\}$ units to a "seed" $\{MO_4\}$ unit. Under this conceptualisation, (aqueous) disassembly releases these $\{MO_3\}$ units supported by H_2O ligands. Subsequent deprotonation of the $\{MO_3(OH_2)\}$ units yields the starting $\{MO_4\}$ units.

However, disassembly in non-aqueous solutions, by necessity, follows a different pathway (Figure 1). Conceptually, we should expect that a solvent molecule (S) could replace a water molecule in the disassembly process described above. After total disassembly of a POM unit in solvent S, we could expect a mixture of "seed" $\{MO_4\}$ units and $\{MO_3S\}$ units in solution. Recombination of these units produces a variety of $\{M_xO_{3x+1}S_y\}$ or $\{M_xO_{3x}S_y\}$ species in solution.

The S ligand would be expected to be significantly more labile than an *oxo* ligand, and thus one might expect this species to be more amenable to ligand exchange (particularly towards O-donor ligands such as phosphonates, arsonates or carboxylates). Moreover, intramolecular dehydration of $\{M_xO_{3x+1}S_y\}$ or $\{M_xO_{3x}S_y\}$ species could still be expected to take place. In particular, expulsion of a water molecule from a $\{M_xO_{3x}S_y\}$ species could generate a highly unusual $\{M_xO_{3x-1}\}$ fragment supported by solvent molecules. This might be particularly expected if the solvent S is protic, and could transfer protons to *oxo*- ligands to generate H_2O ligands.

The key point is that these fragments are fundamentally different from those that generally form through aqueous bottom-up assembly approaches. Hence, top-down approaches incorporating distinct assembly, disassembly and reassembly processes can access POM structures that would otherwise be impossible to synthesise.

This analysis is consistent with our recently reported analysis of the Lindqvist hexamolybate, $[Mo_6O_{19}]^{2-}$, in methanol.[33] Electrospray ionisation mass spectrometry (ESI-MS) demonstrated the disassembly of the parent POM into a series of methanol or methoxy-supported $\{Mo_xO_{3x}\}$ species (x = 1 or 2), and at least one $\{Mo_xO_{3x-1}\}$ species, $[Mo^{VI}_2O_5(OMe)_3]^-$. Subsequent reassembly of these species in the presence of organophosphonate ligands and Cu^{II} ions produced hybrid TMS-POM species containing phosphonate-supported $\{Mo^{VI}_2O_5(OMe)_2\}$ and $[Mo^{VI}_3O_8(OMe)_2\}$ moieties – thus demonstrating the utility of top-down synthetic methods to introduce organic ligands and generate novel TMS-POMs.[33]

Given that this methodology can generate otherwise-inaccessible fragments, we propose that "top-down" synthetic conditions may be used as a *starting point* for the synthesis of new POM materials. If a POM species is known to disassemble under certain conditions, these conditions can provide starting points for explorative attempts at reassembly into novel materials. We expect that the reassembly process would be significantly influenced by the presence of structure-directing species such as ligands or heterometals. While this technique does not have the predictability of, say, the more systematic lacunary approach, it could serve as potentially fertile ground for generating unforeseen structures.

Hybrid $\{Mo_{10}Co_6\}$ structures

Following on from our previously reported disassembly-reassembly approach to generate hybrid Cu^{II}/Mo^{VI} compounds from Lindqvist hexamolybdate $[Mo_6O_{19}]^{2-}$, we turned our attention to the synthesis of mixed-metal Co/Mo compounds.[33] For this purpose, the Lindqvist hexamolybdate was dissolved in acetonitrile in the presence of cobalt (II) acetate and *tert*-butylphosphonic acid. It was anticipated that the combination of heterometal ions, acetate and phosphonate ligands would provide suitable templates for the reassembly of any molybdate fragments formed in solution. Pyridine was also added to act as a base for the phosphonic acid, along with excess tetrabutylammonium salt to promote crystallisation.

Compound **1**, $[TBA]_2[Mo^{VI}_{10}Co^{II}_6O_{12}(\mu\text{-}O)_{14}(\mu_3\text{-}O)_4(t\text{BuPO}_3)_6(\text{MeCOO})_2(\text{py})_2(H_2O)_6]$, was isolated from this reaction mixture as magenta crystals (TBA represents tetrabutylammonium, *t*Bu represents the *tert*-butyl moiety, and py represents pyridine). The structure of **1** was solved and refined in the monoclinic space group $P2_1/n$ along with three constituent acetonitrile solvent molecules per formula unit. X-ray diffraction analysis reveal that the mixed metal cluster in the compound consists of two $\{Mo_5\}$ units sandwiching a core of six Co^{II} centres (Figure 2). This structure can only be synthesised by a top-down method involving *in situ* disassembly and reassembly of the Lindqvist hexamolybdate, and cannot be accessed *via* bottom-up approaches alone (see discussion below).

Each $\{Mo_5\}$ unit can be subdivided into four $\{MoO_6\}$ octahedra and one $\{MoO_4\}$ tetrahedron. The edge-sharing $\{MoO_6\}$ octahedra are linked into a bend arrangement *via* three μ_2-O linkers and a capping phosphonate ligand which coordinates to all four centres in a $\eta^1{:}\eta^1{:}\eta^2{:}\mu_4$ binding mode. Six terminal *oxo*-ligands further stabilise the octahedrally coordinated Mo centres. The Mo centre with a tetrahedral coordination environment is located on the opposite face of the bend arrangement from the phosphonate, linking to the each of the four other Mo centres *via* two μ_3-O linkers, which

View Article Online
DOI: 10.1039/C9DT00075E

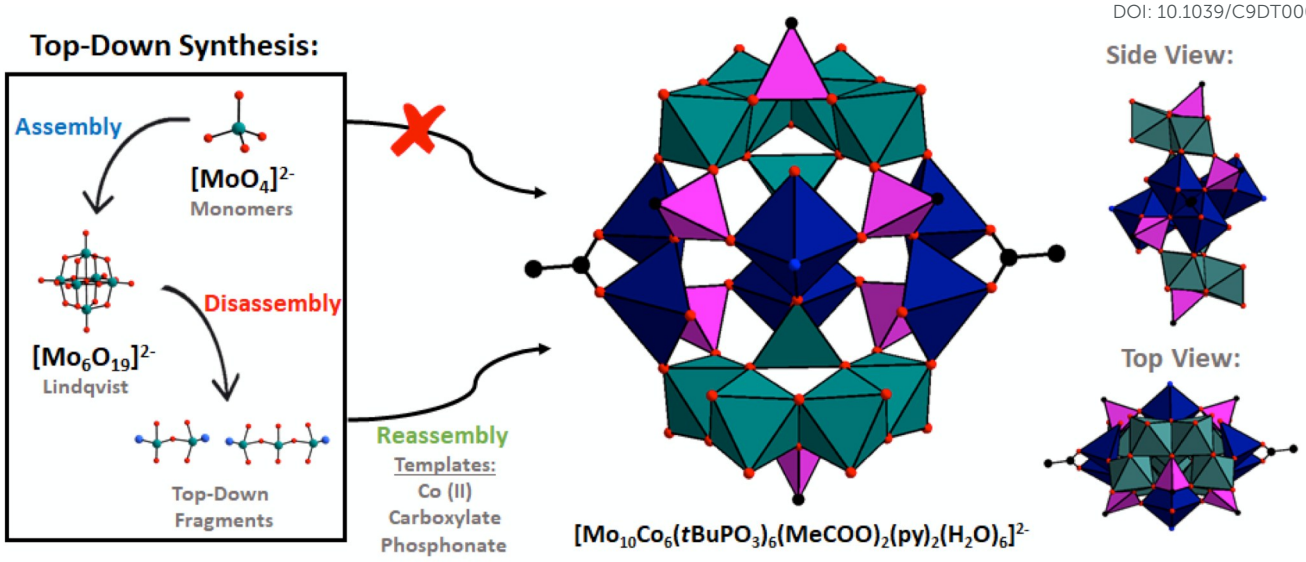

Figure 2. The top-down synthetic approach was used to access compound **1**, [TBA][$Mo_{10}Co_6O_{30}$(*t*BuPO_3)$_6$(MeCOO)$_2$(py)$_2$(H_2O)$_6$], which cannot be accessed by bottom-up approaches alone. Stereoscopic views of the anionic cluster core of **1** are presented. Colour scheme: Mo teal polyhedra, Co dark blue polyhedra, P pink polyhedral, O red, C black. For clarity, *tert*-butyl groups and pyridine ligands are reduced to a single C or N atom, respectively. H atoms are omitted.

form mutual corners between the {MoO_4} tetrahedron and all four of the {MoO_6} octahedra. Four additional μ_2-O linkers and four additional phosphonate ligands, all of which link the {Mo_5} unit to Co centres in the sandwich core, complete the {Mo_5} unit. Bond Valence Sum (BVS) analysis is consistent with Mo^{VI} oxidation states. Bond lengths range from the short terminal Mo-O bonds (*ca.* 1.7 Å) to the long Mo-phosphonate bonds (> 2.2 Å, see ESI for further information).

The cobalt (II) core of the sandwich-type structure can be subdivided into two pairs of dinuclear Co^{II} units and two isolated Co octahedra. The dinuclear unit is bridged by two μ-O phosphonate donors, and one peripheral acetate ligand. The geometry of both centres is distorted square pyramidal, with acetate O donors forming the apex of each pyramid, and phosphonate O donors forming a shared edge between the two pyramids. The acetate ligand binds to each metal centre in the dinuclear unit in a *syn, syn*- bidentate bridging mode. Each dinuclear unit is linked to two {Mo_5} units *via* two μ_2-O linkers on opposite ends of the unit, which both bridge to octahedral Mo sites. Aqua ligands (one on each Co^{II} centre) complete the {CoO_5} coordination spheres.

The two remaining Co^{II} centres are isolated from the other Co^{II} centres, adopting {CoO_5N} octahedral coordination environments. The isolated Co centres are each linked to two {MoO_4} tetrahedra from the {Mo_5} units *via* two μ-O linkers in a *cis*-configuration. Each centre is additionally linked to both of the dinuclear units *via* two phosphonate ligands, which coordinate monodentate O-donors to the metal centre in a *trans*- configuration. The coordination sphere is completed by one aqua ligand and one pyridine ligand. BVS analysis indicates the Co centres are all in oxidation state +II, with Co-O bond lengths in the range of *ca.* 2.0–2.2 Å.

Each face of the {$Mo_{10}Co_6$} cluster in **1** is covered in an intramolecular hydrogen bonding network, with the terminal aqua ligands (one on each Co centre) engaging in hydrogen bonding with phosphonate O-donors or with terminal *oxo*-ligands (see ESI). This network of weak H-O interactions may help stabilise this molecular structure relative to other potential configurations, thus playing a role in determining the molecular structure of the product.

Orthogonal Ligand Substitution

In total, two pyridine, two bridging acetate and six bridging phosphonate ligands stabilise the cluster core of **1**. The pyridine and carboxylate ligands stabilise only Co^{II} centres, with the carboxylates bridging between the Co^{II} centres to form the the dinuclear unit. Two of the phosphonate ligands stabilise only Mo centres in a η^1:η^1:η^2:μ_4 binding mode. The other four phosphonates each bridge between an {Mo_5} unit, a dinuclear Co unit and another Co centre in a η^1:η^1:η^2:μ_4 binding mode.

It was hypothesised that the various organic moieties could be used as synthetic handles to allow modification of the structure (Figure 3, Tables 1 and 2). Modification of the supporting ligands could potentially allow manipulation of the cluster properties or incorporation of the clusters into more complicated architectures.

View Article Online
DOI: 10.1039/C9DT00075E

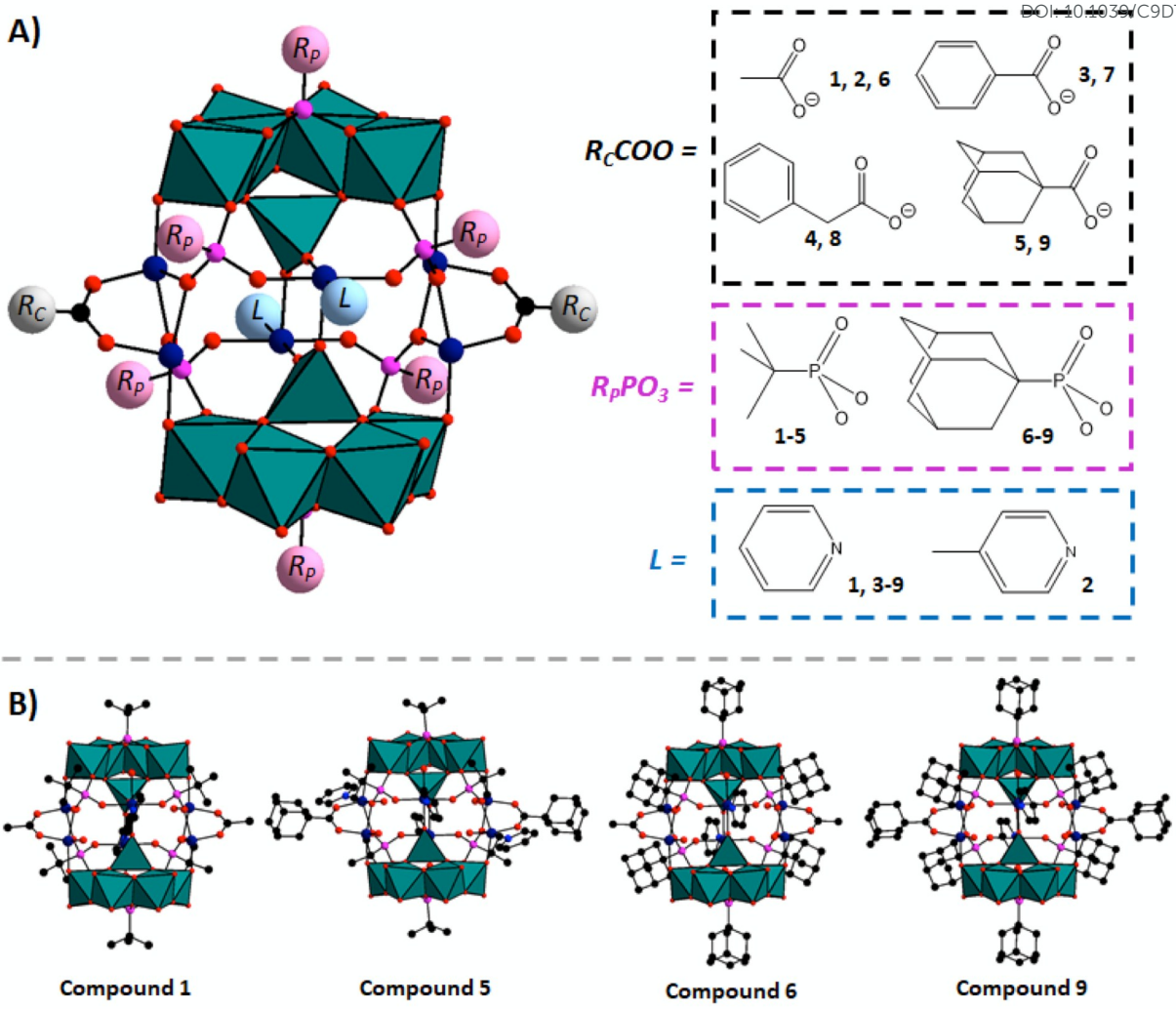

Figure 3. a) The three distinct classes of organic ligand present in compound **1** – pyridyl, carboxylate and phosphonate ligands – can be replaced by equivalent ligands to generate a series (**1 – 9**) of related cluster compounds. Each class of ligand can be independently substituted without affecting the other ligands. **B)** A selection of compounds showing organic ligands of varying bulk present on the cluster core.

In a simple demonstration of this principle, $[TBA]_2[Mo^{VI}_{10}Co^{II}_6O_{30}(t\text{BuPO}_3)_6(\text{MeCOO})_2(\text{picoline})_4(H_2O)_6]$, **2**, was prepared. As expected, **2** is the picoline substituted analogue of **1**, as confirmed by X-ray diffraction analysis. Like in **1**, the cluster core in **2** contains two {Mo_5} units sandwiching six Co^{II} centres stabilised by bridging *tert*-butylphosphonate ligands. The only significant structural difference between **1** and **2** is that one of the Co^{II} centres in each of the dinuclear units expands its coordination sphere, incorporating an additional picoline ligand to generate a distorted octahedral {CoO_5N} environment (see ESI). The structure of **2,** along with 4.4 acetonitrile solvent molecules per formula unit, was solved and refined in the triclinic space group $P\bar{1}$.

Having demonstrated the principle of modification, a series of substitutions at the carboxylate position were carried out (Figure 3, Tables 1 and 2). Compound **3**, $[TBA]_2[Mo^{VI}_{10}Co^{II}_6O_{30}(t\text{BuPO}_3)_6(\text{PhCOO})_2(\text{py})_4(H_2O)_6]$, was generated using benzoate ligands in place of acetate ligands. **3** was solved and refined in the monoclinic space group *C*2/c. No constitutional solvent molecules were observed either crystallographically or through thermogravimetric analysis.

$[TBA]_2[Mo^{VI}_{10}Co^{II}_6O_{30}(t\text{BuPO}_3)_6(\text{BzCOO})_2(\text{py})_2(H_2O)_6]$, **4**, incorporates phenylacetate ligands at the carboxylate position. Structural flexibility around the CH_2 linker does not disrupt crystallisation, with **5** crystallising in the monoclinic space group $P2_1/n$ along with 3.5 acetonitrile molecules. Similarly, compound **5**, $[TBA]_2[Mo^{VI}_{10}Co^{II}_6O_{30}(\text{AdCOO})_2(t\text{BuPO}_3)_6(\text{py})_4(H_2O)_6]$, can be synthesised using adamantylcarboxylate (AdCOO) ligands. Compound **5** crystallised in the monoclinic space group *C*2/*c*, with no constitutional solvent molecules observed. **1**-**5** demonstrate that the carboxylate binding position is reasonably tolerant and carboxylate ligands with varying bulk and flexibility can selectively be introduced.

View Article Online DOI: 10.1039/C9DT00075E

Table 1. Crystallographic details for compounds **1 – 5**.

Compound	**1** ·3(MeCN)	**2** · 4.4(MeCN)	**3**	**4** ·3.5(MeCN)	**5**
Formula	$Mo_{10}Co_6P_6O_{58}$ $N_7C_{76}H_{163}$	$Mo_{10}Co_6P_6O_{58}$ $N_{10.4}C_{92.8}H_{185.2}$	$Mo_{10}Co_6P_6O_{58}$ $N_6C_{90}H_{167}$	$Mo_{10}Co_6P_6O_{58}$ $N_{7.5}C_{89}H_{172.5}$	$Mo_{10}Co_6P_6O_{58}$ $N_6C_{98}H_{176}$
Weight (g mol^{-1})	3601.92	3873.7	3910.7	3773.82	3865.24
Crystal System	Monoclinic	Triclinic	Monoclinic	Monoclinic	Monoclinic
Space Group	$P2_1/n$	$P\bar{1}$	$C2/c$	$P2_1/n$	$C2/c$
Z	2	1	4	2	4
a (Å)	14.9997(4)	13.9147(6)	21.7038(18)	15.6966(7)	22.2697(15)
b (Å)	25.6304(7)	17.0418(7)	24.446(2)	19.5580(9)	24.3823(17)
c (Å)	17.4332(5)	17.3781(7)	28.467(3)	23.4785(10)	28.6484(18)
α (°)	90	74.837(1)	90	90	90
β (°)	96.010(1)	80.331(1)	109.836(1)	97.587	110.0166(17)
γ (°)	90	83.527(2)	90	90	90
Volume (Å^3)	6665.3(3)	3910.7(3)	14208(2)	7144.7(6)	14616.1(17)
Temperature (K)	100(2)	100(2)	100(2)	100(2)	100(2)
μ (mm^{-1})	1.786	1.529	1.680	1.671	1.635
Data/Parameters	28146/779	23891/923	17629/671	20165/866	16792/858
Goodness of Fit	1.006	1.093	1.079	1.193	1.086
R_{int}	0.0416	0.0618	0.0464	0.0738	0.0692
R_1 [I > 2σ(I)]	0.0302	0.0460	0.0615	0.0514	0.0563
wR_2	0.0731	0.1089	0.1584	0.1041	0.1383

To investigate the substitution of **1** at the phosphonate positions, the synthesis of **1** was repeated with adamantylphosphonic acid in place of *tert*-butylphosphonic acid. Compound **6**, $[TBA]_2[Mo^{VI}_{10}Co^{II}_6O_{30}(AdPO_3)_6(MeCOO)_2(py)_2(H_2O)_6]$, crystallised from this reaction mixture. The crystal structure of **6** was solved and refined in the monoclinic space group $P2_1/n$. This demonstrates that the compounds can be successfully substituted at the phosphonate position.

Compound **7**, $[TBA]_2[Mo^{VI}_{10}Co^{II}_6O_{30}(AdPO_3)_6(PhCOO)_2(py)_2(H_2O)_6]$, was synthesised using adamantylphosphonate and benzoate ligands. The structure of **7** was solved and refined in the monoclinic space group $C2/m$. **7** is equivalent to the adamantlyphosphonate-substituted analogue of **3** or the benzoate-substituted analogue of **6**. Similarly, compound **8**, $[TBA]_2[Mo^{VI}_{10}Co^{II}_6O_{30}(AdPO_3)_6(BzCOO)_2(py)_3(H_2O)_6]$, was synthesised using adamantylphosphonate and phenylacetate ligands. The structure of **8** was solved and refined in the triclinic space group $P\bar{1}$. Compound **8** contains two crystallographically distinct cluster units, one of which contains two pyridine ligands (analogous to **1**), the other of which contains four (analogous to **2**, see ESI). Therefore, the formula is given as containing three pyridine ligands. Compound **9**, $[TBA]_2[Mo^{VI}_{10}Co^{II}_6O_{30}(AdPO_3)_6(AdCOO)_2(py)_2(H_2O)_6]$, was synthesised using adamantyl-phosphonate and adamantylcarboxylate ligands. The structure of **9** was solved and refined in the triclinic space group $P\bar{1}$. **8** and **9** represent the adamantylphosphonate analogues of **4** and **5**, respectively.

Table 2. Crystallographic details for compounds **6 – 10**.

Compound	**6** · 9.5(MeCN)	**7** · 2(MeCN)	**8** ·5(MeCN)	**9** ·6(MeCN)	**10** · 7.5(MeCN)
Formula	$Mo_{10}Co_6P_6O_{58}$ $N_{13.5}C_{125}H_{218.5}$	$Mo_{20}Co_{12}P_{12}O_{116}$ $N_{12}C_{240}H_{354}$	$Mo_{10}Co_6P_6O_{58}$ $N_{10}C_{133}H_{203}$	$Mo_{10}Co_6P_6O_{58}$ $N_{10}C_{136}H_{130}$	$Mo_5Co_3P_3O_{29}$ $N_{5.75}C_{45.5}H_{87.25}$
Weight (g mol^{-1})	4337.42	8260.93	4368.84	4331.29	1928.36
Crystal System	Monoclinic	Monoclinic	Triclinic	Triclinic	Triclinic
Space Group	$P2_1/n$	$C2/m$	$P\bar{1}$	$P\bar{1}$	$P\bar{1}$
Z	2	2	2	1	2
a (Å)	17.6667(8)	29.7884(13)	17.7506(7)	16.9115(8)	13.7500(4)
b (Å)	25.3666(12)	28.1953(12)	18.8983(8)	17.8098(9)	16.8554(5)
c (Å)	20.0291(9)	19.9483(8)	27.1892(12)	18.2776(9)	17.1095(5)
α (°)	90	90	75.8350(10)	65.2690(10)	107.6320(10)
β (°)	107.6720(10)	91.4630(10)	80.8820(10)	64.0720(10)	95.0120(10)
γ (°)	90	90	75.5210(10)	84.8630(10)	101.6640(10)
Volume (Å^3)	8552.3(7)	16749.0(12)	8399.5(6)	4467.4(4)	3653.79(19)
Temperature (K)	100(2)	100(2)	100(2)	100(2)	100(2)
μ (mm^{-1})	1.409	1.433	1.435	1.349	1.636
Data/Parameters	16945/106	16357/938	34616/1956	24963/971	22705/848
Goodness of Fit	0.889	1.068	1.009	1.022	1.002
R_{int}	0.0909	0.0738	0.0895	0.0528	0.0889
R_1 [I > 2σ(I)]	0.0356	0.0698	0.0439	0.0622	0.0544
wR_2	0.0643	0.1668	0.0957	0.1622	0.0903

View Article Online
DOI: 10.1039/C9DT00075E

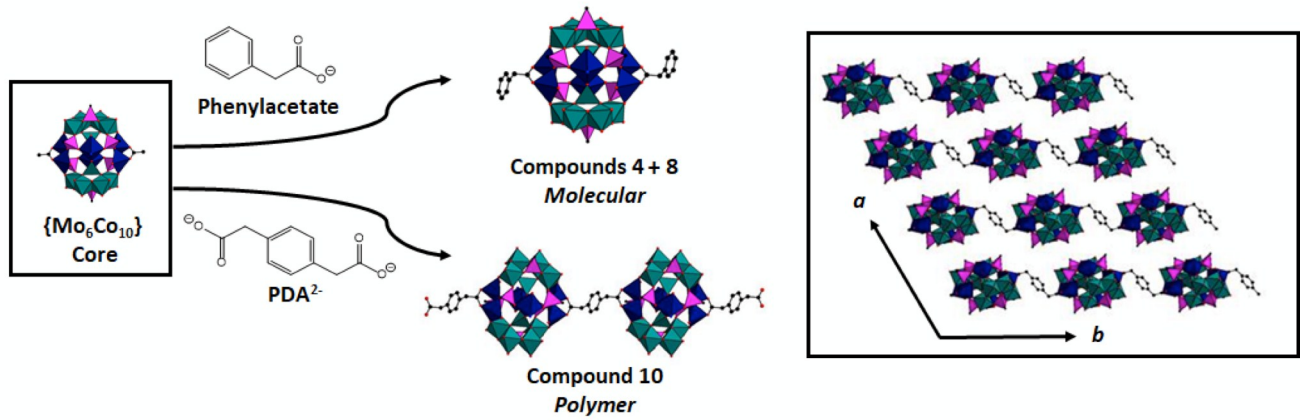

Figure 4. Phenylacetate ligands generate the molecular compounds **4** and **8**, while the ditopic analogue PDA^{2-} generates compound **10**, a one dimensional hybrid metallopolymer compound. *Inset*: A portion of the crystal structure of compound **10**, showing the propagation of polymer chains along the crystallographic *b*-axis. Solvent molecules and cations are removed for clarity.

The series **1–9** have a range of supporting organic ligands with varying bulk and flexibility. This indicates that the synthetic procedure is reasonably robust and versatile, which may allow for inclusion of more complicated functional moieties at the carboxylate binding site. Moreover, substitutions at any one of the ligand sites (pyridyl, carboxylate or phosphonate) do not affect substitution at any other site. This provides an additional layer of flexibility to the system, as selective substitution at distinct ligand sites allows different functional groups to be attached to the cluster core in an orthogonal manner.

1D polyoxometalate-based coordination polymer

Hybrid POM compounds are sought-after synthetic targets in part because of the possibility of incorporating POM units into supramolecular polymer or framework structures.[6–10] The $\{Mo_{10}Co_6\}$ cluster core in the compounds was thought to be an ideal platform for assembly into polymeric materials using polytopic ligands. One synthetic constraint is the requirement that the polytopic ligand does not readily form polymeric or framework materials with Co^{II} ions. The $\{Mo_{10}Co_6\}$ compounds crystallise over a period of weeks; any cobalt coordination polymer which forms more readily will sequester the Co^{II} ions from solution and prevent formation of the $\{Mo_{10}Co_6\}$ compound.

Therefore, phenylenediacetic acid (H_2PDA) was chosen as a suitable linker ligand to facilitate the formation of a 1D-chain structure based on hybrid POM species. PDA^{2-} alone does not sequester Co^{II} ions from solution, and the ligand is rotationally flexible, allowing a 1D chain structure to find a favourable packing arrangement. The use of H_2PDA in this reaction system produced crystals of compound **10**, $[TBA]_2[Mo^{VI}_{10}Co^{II}_6O_{30}(t\text{BuPO}_3)_6(PDA)(py)_2(H_2O)_6]$, which crystallised over the course of approximately one month. The structure was solved and refined in the monoclinic space group $P\bar{1}$. Hybrid polymer chains propagate throughout the crystal structure along the crystallographic *b*-axis (Figure 4).

We believe that rotational flexibility around the methylene spacers in the PDA linker is important to isolation and crystallisation of the polymer species. In the molecular species **4** and **8**, the O-C-C-Ph torsion angles of the phenylacetate adopt values up to *ca*. 45°. However, in **10,** the equivalent angle increases to 83°. We attribute this difference to packing constraints – with two close-to-perpendicular torsion angles, the PDA linker effectively acts as an (offset) linear linker between $\{Mo_{10}Co_6\}$ cluster units.

The isolation of polymer **10** demonstrates that the top-down approach can be used to generate both molecular and polymeric compounds. Moreover, the phosphonate and pyridyl ligands remain as synthetic handles for further functionalisation of the material. Future work will explore the addition of functional groups onto the organic ligands, which will provide an avenue towards both manipulation of the electronic properties of the Co^{II} centres, as well as post-synthetic modification of the cluster into more sophisticated supramolecular architectures.

Templating effects in top-down synthesis of POMs

The $\{Mo_5O_{15}\}$ unit in compounds **1–10** is extremely unusual, only appearing in one manganese-molybdenum compound previously reported by us.[34] In particular, the presence of a tetrahedral $\{MoO_4\}$ centre within an extended POM structure is unusual. Although not immediately obvious, the unit does bare structural similarities to both the α-octamolybdate and the Strandberg ring structures (Figure 5). In both of these compounds, a ring structure is templated on either side by either $\{MoO_4\}$ or phosphonate templating species. As has been discussed elsewhere, ring structures like these are probably kinetic products (chain structures are known to form

View Article Online
DOI: 10.1039/C9DT00075E

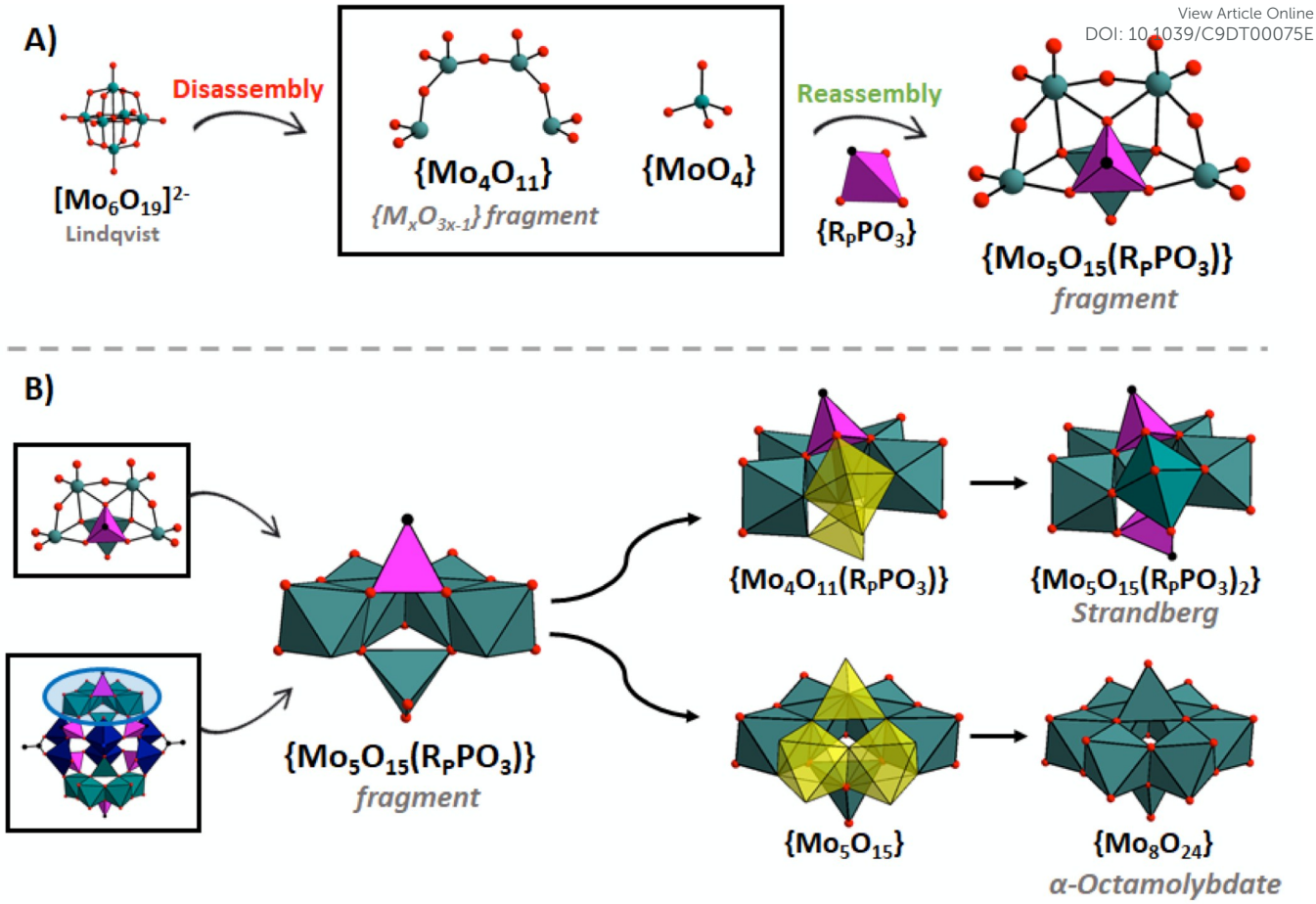

Figure 5. A) The proposed assembly of a the $\{Mo_5\}$ molybdate fragments in **1**-**10** from a phosphonate ligand, a tetrahedral $\{MoO_4\}$ unit, and a $\{Mo_4O_{11}\}$ unit. The latter unit could only have been generated from a top-down disassembly process, and could not have formed by a bottom-up assembly process alone. B) Schematic relating the $\{Mo_5\}$ unit to the ring structures seen in the Strandberg and α-octamolybdate compounds.

more rapidly than dense phases, and simple templates will promote ring formation from oligomeric chains).[16]

We propose that the $\{Mo_5\}$ unit in **1–10** forms from the assembly of a tetrameric $\{Mo_4O_{11}\}$ unit, templated into a partial ring structure by an $\{MoO_4\}$ tetrahedron on one side and a phosphonate ligand on the other (Figure 5). Notably, this requires a $\{M_xO_{3x-1}\}$ fragment to form, which is only accessible by a top-down synthetic procedure (*c.f.* Figure 1).

While an $\{Mo_5O_{15}\}$ unit could, in principle, be generated by a purely bottom-up approach, this unit has not yet been observed from a classical POM synthesis. Moreover, a simple substitution of sodium molybdate (Na_2MoO_4) in place of the Lindqvist hexamolybdate does not yield the desired products, instead generating a blue powder. This powder was not fully characterised, but on the basis of IR data (see ESI) appears to consist primarily of a cobalt-phosphonate compound. This result indicates that the $\{Mo_5O_{15}\}$ unit does not directly form in a bottom-up manner under our chosen synthetic conditions. While we do not rule out the possibility that this unit could form under modified conditions, it seems clear that under our synthetic regime at least, a top-down synthetic process is necessary to achieve the desired products. The proposed combination of $\{Mo_xO_{3x-1}\}$ fragments, $\{MoO_4\}$ species, and phosphonate ligands can only be present under a top-down synthetic regime consisting of distinct assembly, disassembly and reassembly processes.

Conclusions

In summary, the "top-down" synthetic methodology is potentially useful but underexplored avenue towards new hybrid, mixed-metal polyoxometalate (POM) compounds. This methodology involves distinct assembly, disassembly and reassembly processes, which generate a series of synthetic fragments that are inaccessible *via* direct bottom-up assembly. In this account, we outline the key characteristics of this approach and apply it to the generation of ligand-supported Co^{II}/Mo^{VI} compounds. The applied methodology involves the assembly of a classical Lindqvist hexamolybdate, $[Mo_6O_{19}]^{2-}$, disassembly of the POM into reactive fragments in acetonitrile solution, and reassembly of these fragments into hybrid, TMS-POM compounds.

These compounds have a general formula $[TBA]_2[Mo^{VI}_{10}Co^{II}_6O_{30}(R_pPO_3)_6(R_cCOO)_2(L)_x(H_2O)_6]$, where TBA

View Article Online
DOI: 10.1039/C8CE00975F

represents tetrabutylammonium, R_p represents an organic phosphonte moiety, R_c a carboxylate moiety, L represents either pyridine or picoline, and x = 2–4. The R_p, R_c and L components can be substituted in an orthogonal manner by simply replacing the relevant ligand to generate a series of ten compounds containing a variety of organic substituents. This series includes nine molecular structures and one 1D coordination polymer, in which the cluster entities are linked into one-dimensional hybrid chains *via* phenylenediacetate linkers. Future work aims to incorporate more sophisticated functional groups onto these organic ligands with the objective of modifying the electronic properties of the clusters and assembling the clusters into more sophisticated supramolecular architectures.

We believe that the top-down approach towards hybrid, TMS-POMs is a potentially fruitful methodology which could generate complex, novel compounds with unforeseen structures. We anticipate that this methodology could spur a new wave of exploratory synthesis of these interesting or structurally related heterometallic compounds.

Experimental

Methods and Materials

Lindqvist hexamolybdate $[TBA]_2[Mo_6O_{19}]$ and adamantylphosphonic acid were synthesised by literature procedures (see ESI). All other reagents were purchased from Sigma-Aldrich, Alfa Aesar or Acros Organics and used without further purification. Single crystal X-ray diffraction analyses were performed using a Bruker APEX2 Duo diffractometer equipped with a sealed-tube Mo-Kα source (λ = 0.71073 Å) and a microfocus Cu-Kα source (λ = 1.5418 Å). Data was gathered using a Bruker SMART APEX2 area detector. Intensity data was processes with APEX3 v2015.9-0 and corrected for absorption by multi-scan methods using SADABS. The structures were solved and refined using SHELXT and SHELXL-2013 as implemented in Olex 2. H positions were calculated using a riding model. Where appropriate, the SQUEEZE routine was used to model disordered solvent molecules. Infrared data in the 4000-650 cm^{-1} region were obtained using a PerkinElmer Spectrum One FT-IR spectrometer with a universal Attenuated Total Reflectance (ATR) sampling accessory. Thermogravimetric analyses were performed using a Perkin Elmer Pyriss 1 TGA instrument that had been previously calibrated using nickel and iron standards. Samples were heated in a ceramic crucible under a nitrogen atmosphere from room temperature to c. 800° C, at a rate of 10° C/min.

General Synthetic Procedure

$[TBA]_2[Mo_6O_{19}]$ (0.068 g, 0.05 mmol), a cobalt (II) carboxylate salt (0.25 mmol), a phosphonic acid (0.25 mmol) and tetrabutylammonium bromide (0.161 g, 0.5 mmol) were combined in acetonitrile (25 ml). Alternatively, cobalt (II) nitrate hexahydrate (0.073 g, 0.25 mmol) and a carboxylic acid (0.5 mmol) could be used. Pyridine or picoline (0.5 mmol) was subsequently added. The solution was stirred at room temperature for four hours with the appearance of a dark purple colour. The purple solution was filtered to remove any solid material, and the solvent was allowed to evaporate slowly until magenta crystals suitable for X-ray diffraction analysis formed (usually 1-2 weeks). The crystals were isolated by filtration, washed with diethyl ether and air dried. In some cases, the crystals were contaminated by an unidentified, insoluble dark blue solid; in these instances the solids were re-dissolved in acetonitrile, the blue solid removed by filtration, and the crystallisation procedure repeated. Analytical data for **1–10** can be found in the ESI. Crystallographic data can be obtained from The Cambridge Crystallographic Data Centre (**1876736** - **1876745**) *via* www.ccdc.cam.ac.uk /data_request/cif.

Conflicts of interest

There are no conflicts to declare.

Acknowledgements

The authors thank Science Foundation Ireland (SFI; 13/IA/1896), the European Research Council (CoG 2014 – 647719) and the Irish Research Council (Fellowship for C.H.) for financial support. We thank Dr. Brendan Twamley for X-ray diffraction measurements and analyses.

Notes and references

§ In order to distinguish these processes from traditional, purely bottom-up approaches, we apply the top-down label to any system where disassembly of a POM species occurs, even if combinations of bottom-up assembly and top-down disassembly take place.

1 a) P. Gouzerh and M. Che, *Actual. Chim.*, 2006, **298**, 9; b) M. Mirzaei, H. Eshtiagh-Hosseini, M. Alipour and A. Frontera, *Coord. Chem. Rev.*, 2014, **275**, 1; c) S. Taleghani, M. Mirzaei, H. Eshtiagh-Hosseini and A. Frontera, *Coord. Chem. Rev.*, 2016, **309**, 84; d) Celebrating Polyoxometalates Special Issue, *Eur. J. Inorg. Chem.,* 2019, 3, 377.
2 S. Wang and G. Yang, *Chem. Rev.*, 2015, **115**, 4893.
3 J. J. Walsh, A. M. Bond, R. J. Forster and T. E. Keyes, *Coord. Chem. Rev.*, 2016, **306**, 217.
4 A. Proust, R. Thouvenot and P. Gouzerh, *Chem. Commun.,* 2008, 1837.
5 A. Proust, B. Matt, R. Villanneau, G. Guillemot, P. Gouzerh and G. Izzet*, Chem. Soc. Rev.,* 2012, **41**, 7605.
6 C. Yvon, A. Macdonell, S. Buchwald, A. J. Surman, N. Follet, J. Alex, D. Long and L. Cronin*, Chem. Sci.,* 2013, **4**, 3810.
7 H. Yang, M. Su, L. Ren, J. Tang, Y. Yan, W. Miao, P. Zheng and W. Wang, *Eur. J. Inorg. Chem*., 2013, 1381.
8 W. Chen, U. Tong, T. Zeng, C. Streb and Y.-F. Song, *J. Mater. Chem. C,* 2015, **3**, 4388.
9 M. Piot, S. Hupin, H. Lavanant, C. Afonso, L. Bouteiller, A. Proust and G. Izzet, *Inorg. Chem.,* 2017, **56,** 8490.
10 Y. Wang, M. Zhang, S. Li, S. Zhang, W. Xie, J. Qin, Z. Su and Y. Lan, *Chem. Commun.,* 2017, **53**, 5204.
11 A. Sartorel, M. Carraro, G. Scorrano, R. De Zorzi, S. Geremia, N. D. McDaniel, S. Bernhard and M. Bonchio, *J. Am. Chem. Soc.*, 2008, **130**, 5006.
12 R. Al-Oweini, A. Sartorel, B. S. Bassil, M. Natali, S. Berardi, F. Scandola, U. Kortz and M. Bonchio, *Angew. Chem. Int. Ed.*, 2014, **53**, 11182.

13 B. Schwarz, J. Forster, M. K. Goetz, D. Yucel, C. Berger, T. Jacob and C. Streb, *Angew. Chem. Int. Ed.,* 2016, **55**, 6344.
14 L. Vilá-Nadal, A. Rodríguez-Fortea, L. K. Yan, E. F. Wilson, L. Cronin and J. M. Poblet, *Angew. Chem. Int. Ed*., 2009, **48**, 5452.
15 L. Vilà-Nadal, S. G. Mitchell, A. Rodríguez-Fortea, H. N. Miras, L. Cronin and J. M. Poblet, *Phys. Chem. Chem. Phys*., 2011, **13**, 20136.
16 L. Vilà-Nadal, E. F. Wilson, H. N. Miras, A. Rodríguez-Fortea, L. Cronin and J. M. Poblet, *Inorg. Chem.,* 2011, **50**, 7811.
17 C. Healy and W. Schmitt, *Coord. Chem. Rev.,* 2018, **371**, 67.
18 R. Al-Oweini, B. S. Bassil, J. Friedl, V. Kottisch, M. Ibrahim, M. Asano, B. Keita, G. Novitchi, Y. Lan, A. Powell, U. Stimming and U. Kortz, *Inorg. Chem*., 2014, **53**, 5663.
19 K. Kastner, J. T. Margraf, T. Clark and C. Streb, *Chem. Eur. J.*, 2014, **20**, 12269.
20 K. Kastner, J. Forster, H. Ida, G. N. Newton, H. Oshio and C. Streb, *Chem. Eur. J.,* 2015, **21**, 7686.
21 J. Hao, Y. Xia, L. Wang, L. Ruhlmann, Y. Zhu, Q. Li, P. Yin, Y. Wei and H. Guo, *Angew. Chem. Int. Ed.,* 2008, **47**, 2626.
22 Y. Huang, J. Zhang, J. Hao and Y. Wei, *Sci. Rep.,* 2016, **6**, 24759.
23 E. F. Wilson, H. Abbas, B. J. Duncombe, C. Streb, D. L. Long and L. Cronin, *J. Am. Chem. Soc.,* 2008, **130**, 13876.
24 E. F. Wilson, H. N. Miras, M. H. Rosnes and L. Cronin, *Angew. Chem. Int. Ed.,* 2011, **50**, 3720.
25 C. P. Pradeep, D. L. Long, C. Streb and L. Cronin, *J. Am. Chem. Soc.,* 2008, **130**, 14946.
26 S. Kodama, N. Taya and Y. Ishii, *Inorg. Chem*., 2014, **52**, 2754.
27 S. Kodama, N. Taya, Y. Inoue and Y. Ishii, *Inorg. Chem*., 2016, **55**, 6712.
28 T. Hoshino, R. Isobe, T. Kaneko, Y. Matsuki and K. Nomiya, *Inorg. Chem*., 2017, **56**, 9585.
29 M. Martin-Sabi, R. S. Winter, C. Lydon, J. M. Cameron, D. Long and L. Cronin, *Chem. Commun*., 2016, **52**, 919.
30 J. Forster, B. Rösner, R. H. Fink, L. C. Nye, I. Ivanovic-Burmazovic, K. Kastner, J. Tucher and C. Streb, *Chem. Sci.,* 2013, **4**, 418.
31 A. Seliverstov and C. Streb, *Chem. Eur. J.,* 2014, **20**, 9733.
32 D. Sures, M. Segardo, C. Bo and M. Nyman, *J. Am. Chem. Soc*., 2018, **140**, 10803.
33 C. Healy, B. Twamley, M. Venkatesan, S. Schmidt, T. Gunnlaugsson and W. Schmitt, *Chem. Commun*., 2017, **53**, 10660.
34 L. Zhang, R. Clérac, C. I. Onet, C. Healy and W. Schmitt, *Eur. J. Inorg. Chem*., 2013, 1654.

View Article Online
DOI: 10.1039/C9DT00075E

Graphical Abstract: